Mechanical Properties and Flammability of Polycarbonate Alloys Containing Nanosize Additives

Zhiyi Zhang, Yaqing Liu, Guizhe Zhao

*Research Center for Engineering Technology of Polymeric Composites of Shanxi Province,
North University of China, Taiyuan 030051, China*

ABSTRACT: Different organic–inorganic composite particles [montmorillonite/poly(butyl acrylate) (PBA)/poly (methyl methacrylate) (PMMA), SiO_2/PBA/PMMA, and $CaCO_3$/PBA/PMMA] were synthesized by emulsion polymerization. Furthermore, polycarbonate (PC) alloys were prepared via the doping of these composite particles into PC with a twin-screw extruder. The structure, mechanical properties, and flammability of the PC alloys were studied in detail. Although the tensile modulus of PC decreased a little, the flexibility and impact resistance were improved by the addition of these composite particles. This result was attributed to the fact that the composite particles were well dispersed in the PC matrix, with a cocontinuous phase formed between the particles and PC. In addition, the combustion behavior of the PC alloys, compared with that of the pure PC, resulted from a ceramic-like char that formed on the surface of the PC alloys during burning. © 2009 Wiley Periodicals, Inc. J Appl Polym Sci 114: 438–445, 2009

Key words: inorganic materials; morphology; polycarbonates; toughness

INTRODUCTION

Polycarbonate (PC) is an important engineering thermoplastic. Because of its excellent clarity, high heat deflection temperature, and good toughness, it is used in a wide range of applications, such as household and consumer articles, sporting goods, photography and optical equipment, and optical-laser data-storage systems.[1–5] However, pure PC may break in a brittle manner because of sharp notches, a high strain rate, plane strain, and low temperatures. This restricts PC's applications in industry. Thus, there are many works about improving the mechanical and thermal properties of PC. PC has been blended with various polymers, such as polyolefins,[6–8] acrylonitrile-butadiene-styrene (ABS),[9–15] styrene copolymers,[16–18] and core–shell rubbers.[19–25] In addition, PC has been blended with thermoplastic elastomers, such as thermoplastic polyurethane,[26,27] poly(ester ether) elastomers,[28] and thermoplastic copolyether ester.[29] Although the impact strength of PC was improved in these works, the bending strength and tensile modulus were reduced. Moreover, these PC alloys are flammable, and this restricts their applications in many cases.

Organic–inorganic composite particles with a core–shell structure have the excellent properties of organic and inorganic materials. An organic polymer encapsulating inorganic particles can improve the dispersion of the inorganic particles in PC and the processability of PC alloys. In another way, inorganic nanoparticles can enhance the strength and flame retardancy of PC alloys.

For these reasons, different inorganic particles [SiO_2, $CaCO_3$, and montmorillonite (MMT)] encapsulating acrylic acid ester were prepared through emulsion polymerization; butyl acrylate (BA) was the soft phase, and methyl methacrylate (MMA) was the hard phase. These composite particles with novel structures were doped into PC, and this resulted in improvements of the tensile strength, impact strength, morphology, processability, thermal properties, and flammability of these PC alloys. These results are very valuable for expanding the applications of PC.

EXPERIMENTAL

Materials

PC (bisphenol A type resin, IR2200) was purchased from Inemitsu Petrochemical Co., Ltd. (Tokyo, Japan). Pristine sodium montmorillonite (Na-MMT) was purchased from Zhejiang Anji Yuhong Clay Chemical Co. (Zhejiang, China), and it had a cationic exchange capacity of 115 mequiv/100 g. Nano-SiO_2 and nano-$CaCO_3$ were purchased from Jiangsu Hehai Nanometer Chemical Co. (Jiangshu, China) MMA and BA were purchased from Beijing Dongfang

Correspondence to: Z. Zhang (zhiyzhang@sohu.com).

Chemical Plant (Beijing, China) and used without further purification. Pristine Na-MMT was dispersed in deionized water for 5 h at 50°C, and then filtration and desiccation were performed before emulsion polymerization. Ammonium persulfate, an initiator, was chemically pure. Sodium dodecyl benzene sulfonate, an emulsifier, was chemically pure. PC was predried at 120°C for 10 h, and acrylic acid ester modifiers were predried at 60°C for 5 h in an air-circulating oven before use.

Preparation of the organic–inorganic composite particles

To a three-necked, round flask equipped with a baffle stirrer and a reflux condenser, 400 mL of deionized water was added after the inletting of nitrogen. Afterward, 10 g of inorganic particles (nano-SiO_2, nano-$CaCO_3$, and Na-MMT) and 0.5 g of an ammonium persulfate aqueous solution were added to a three-necked, round flask at the temperature of 353 K. BA (45 g) was further dropwise added within 30 min. After the reaction of the mixture for 1 h, 45 g of MMA was dropwise added within 30 min. The reaction mixture was left for 3 h. The reaction solution was centrifuged at 1000 rpm for 0.5 h, and the supernatant was removed. The structure of the composite particles was characterized with X-ray diffraction (XRD; X-ray generator operated at 50 kV and 100 mA with Cu Kα; Rigaku) and transmission electron microscopy (TEM; H-600 electron microscope, Hitachi, Japan).

Preparation of the PC alloys

PC/MMT/poly(butyl acrylate) (PBA)/poly(methyl methacrylate) (PMMA), PC/SiO_2/PBA/PMMA, and PC/$CaCO_3$/PBA/PMMA were obtained through the compounding of PC with a 10 wt % modifier that contained different inorganic particles and 5 wt % decabromodiphenyl oxide in a twin-screw extruder (SHJ30, Nanjing Rubber and Plastics Machinery Plant, Nanjing, China; L/Φ = 23, L/Φ is the radio of screw length and screw diameter. The temperature of the extruder was maintained at 250, 260, 265, and 260°C from the hopper to the die. The composites are hereafter called PC/MMT, PC/SiO_2, and PC/$CaCO_3$, respectively. Samples of pure PC and PC with 5 wt % decabromodiphenyl oxide and 10 wt % modifier that did not contain inorganic particles were processed in the same way and were used for comparison; they are hereafter called PC and PC_d.

Characterization of the PC alloys

Mechanical properties

Tensile strength testing was performed with an RGT-10A electronic tensile tester (Shenzhen, China)

with a computer-controlled system. The testing portion of the dumbbell specimen was 25 mm long with a cross section of 2 × 6 mm^2. The test was conducted at an extension rate of 20.0 mm/min at 23°C and 50% relative humidity. The notched impact strength was carried out on an XCJ-40 Charpy impact tester (Hebei, China).

Dynamic mechanical measurements were carried out with a Netzsch (Selb/Bavana, Germany) DMA242 dynamic mechanical analyzer. The measuring frequency was 1 Hz, the bar type specimens were molded at 230°C with dimensions of 40 × 10 × 0.75 mm^3 with a hot press, and the heating rate was 5°C/min. The temperature testing range was −100 to 180°C.

Processability

Processability was determined with a Brabender twin-screw extruder (Lab Station, Duisburg, Germany), which was used for the melt blending of PC and thermoplastic acrylic acid ester modifiers in a 90 : 10 weight ratio. The total mass was 50 g. The processing temperature was 230°C, and the screw speed was 25 rpm.

Distribution

Scanning electron microscopy (SEM) experiments were performed with a TMS-2 scanning electron microscope (Perkin-Elmer, Waltham, MA). SEM samples were prepared by low-temperature fracturing directly before surface coating with gold.

Combustion

Combustion experiments were performed in a cone calorimeter (Fire Testing Technology, West Sussex, United Kingdom) at an incident heat flux of 35 kW/m^2. The peak heat release rate (HRR), effective heat
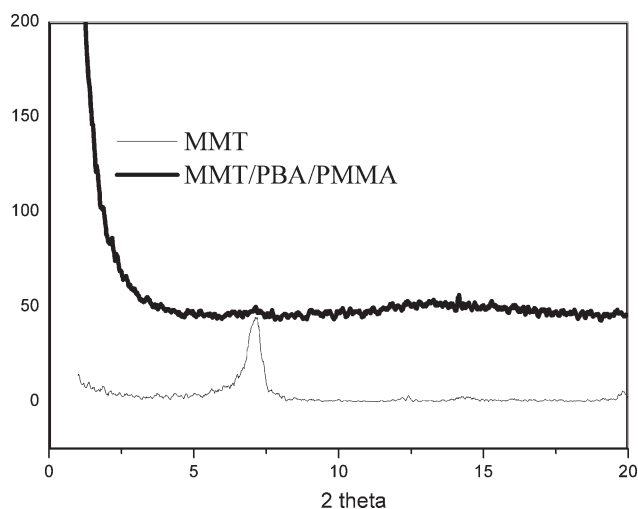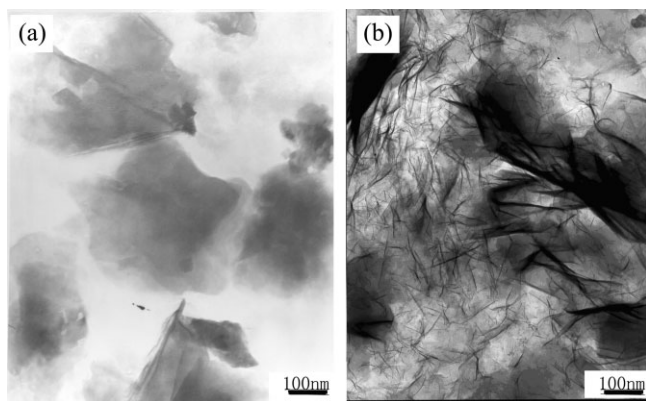

Figure 1 Wide-angle XRD patterns.

Figure 2 Transmission electron micrographs of (a) MMT and (b) MMT/PBA/PMMA.

combustion, total heat evolved, specific extinction area, CO, and CO_2 yield data were reproducible to within 10% tolerance when measured at 35 kW/m² flux.

Char surface

The char surface of the nanocomposites (PC/MMT, PC/SiO$_2$, and PC/CaCO$_3$) was characterized with SEM. The surfaces were coated with gold, and the accelerating voltage was 10 kV.

RESULTS AND DISCUSSION

Preparation of the composite particles

The XRD patterns of Na-MMT and MMT/PBA/PMMA are compared in Figure 1. It shows a peak at $2\theta = 6.97°$, which can be attributed to the XRD pattern of Na-MMT. After emulsion polymerization, MMT interlayer spacing could not be detected, and the peak disappeared, as shown in Figure 1. The TEM patterns of Na-MMT and MMT/PBA/PMMA are compared in Figure 2. It shows that the struc-
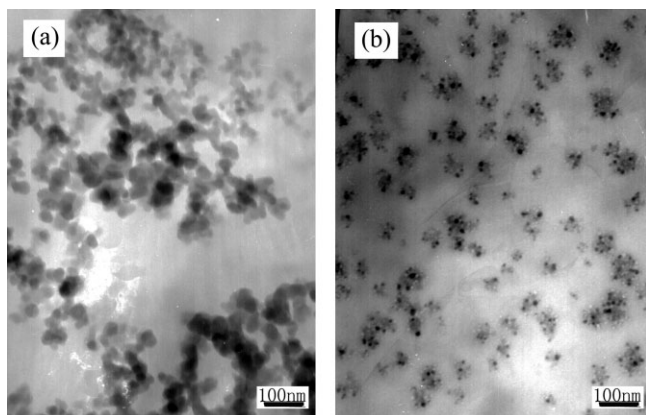

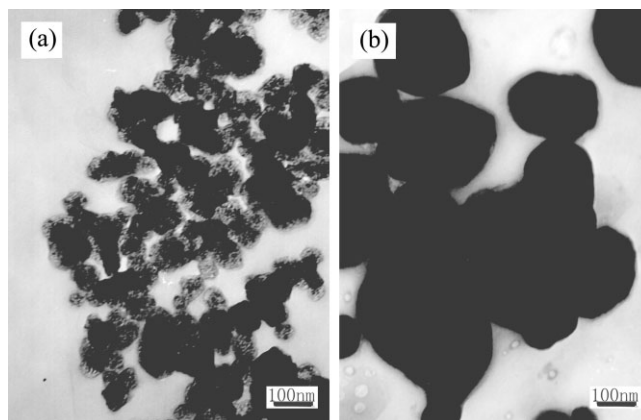**Figure 3** Transmission electron micrographs of (a) SiO$_2$ and (b) SiO$_2$/PBA/PMMA.

Figure 4 Transmission electron micrographs of (a) CaCO$_3$ and (b) CaCO$_3$/PBA/PMMA.

tures of Na-MMT and MMT/PBA/PMMA were evidently different. After emulsion polymerization, the MMT was exfoliated. The results indicate that the MMT was well encapsulated by the polymer.

Figures 3 and 4 display the TEM patterns of SiO$_2$/PBA/PMMA and CaCO$_3$/PBA/PMMA, respectively. SiO$_2$ and CaCO$_3$ were easily aggregated before emulsion polymerization. After emulsion polymerization, there were few aggregate. The results also indicate that CaCO$_3$ and SiO$_2$ were well encapsulated by the polymer. A comparison of Figures 3(b) and 4(b) shows that CaCO$_3$/PBA/PMMA was much larger than SiO$_2$/PBA/PMMA. The reason cannot be explained now.

Mechanical properties

The mechanical properties of the PC and PC alloys are compared in Table I. It shows that the impact strength of PC alloys containing various composite particles increased with the addition of composite particles. The increase was especially obvious for PC$_d$. However, the bending strength and tensile strength evidently decreased with the addition of composite particles. The result can be attributed to the fact that PC$_d$ did not contain inorganic nanoparticles. When these modifiers without inorganic nanoparticles were blended with PC, the impact strength

TABLE I
Mechanical Properties of the PC and PC Alloys

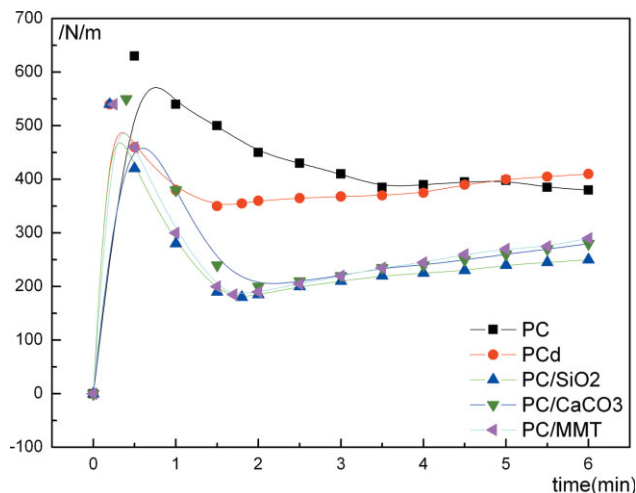| Sample	Bend strength (MPa)	Tensile strength (MPa)	Impact strength (kJ/m²)
PC	104	53	73
PC$_d$	85	42	120
PC/SiO$_2$	98	59	115
PC/MMT	98	58	109
PC/CaCO$_3$	107	56	95

Figure 5 Processability sketch of the PC and PC alloys. [Color figure can be viewed in the online issue, which is available at www.interscience.wiley.com.]

increased, but the bending strength and tensile modulus decreased. It is interesting that through the addition of inorganic nanoparticles to a thermoplastic modifier, the impact strength increased, and at the same time, other mechanical performances hardly decreased. This can be attributed to the fact that the inorganic nanoparticles were a framework for the thermoplastic modifiers and increased the rigidity of the thermoplastic modifiers. It can be concluded that the inorganic particles increased the strength of the PC alloys and that the acrylic ester polymer increased the toughness of the PC alloys.

Processability

Figure 5 shows a processability sketch of the PC and PC alloys. From the sketch, we can see that the maximum torsion and balance torsion of the PC alloys
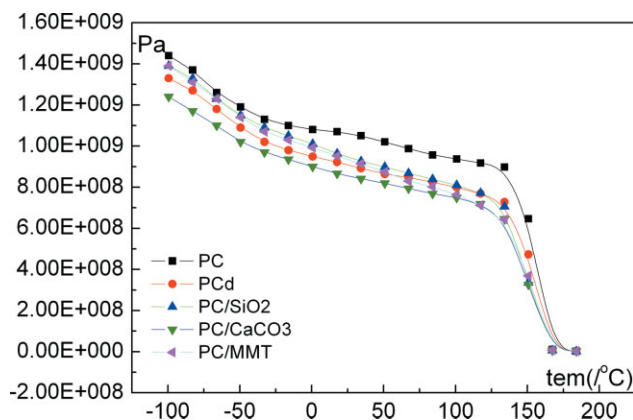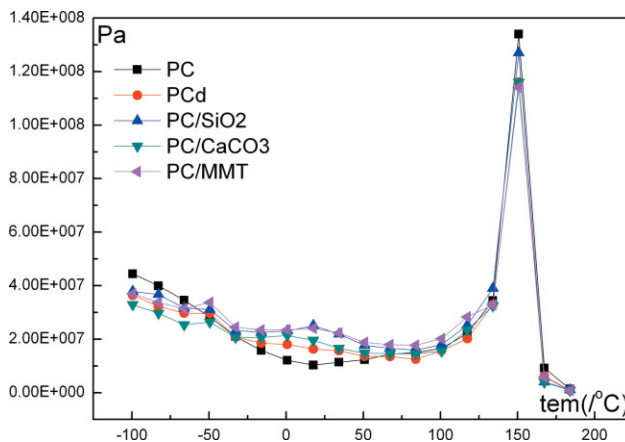

Figure 7 G'' of the PC and PC alloys. [Color figure can be viewed in the online issue, which is available at www.interscience.wiley.com.]

were lower than those of pristine PC, and the time at which balance torsion was reached was shortened; this indicated that the processability of the PC alloys was improved with the addition of these modifiers. These modifiers containing inorganic nanoparticles had better processability and lower viscosity than the modifier without inorganic nanoparticles. The inorganic particles could improve the PC processability. All these PC alloys could be processed at a lower temperature and a higher screw speed.

Dynamic mechanical analysis

The dynamic mechanical properties of the PC and PC alloys are shown in Figures 6–8. The dynamic storage modulus (G') as a function of temperature is illustrated in Figure 6. The magnitude and nature of the change in G' depended on the overall
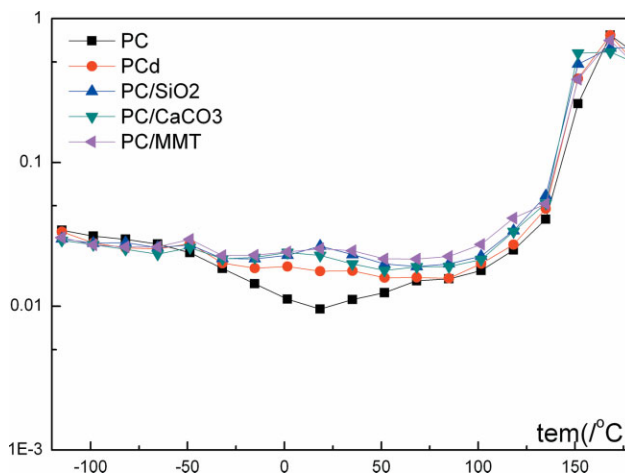

Figure 6 G' of the PC and PC alloys. [Color figure can be viewed in the online issue, which is available at www.interscience.wiley.com.]

Figure 8 Tan δ (G''/G' ratio) of the PC and PC alloys. [Color figure can be viewed in the online issue, which is available at www.interscience.wiley.com.]

composition of the polymer blends and were determined by both the intermolecular and intramolecular interactions; the latter had a greater influence on the different physical states of the polymer.[30] When the modifier was added to the PC matrix, G' of the blends decreased. The modifier was introduced into the rigid PC matrix, the flexibility of which was improved; this resulted in the reduction of G'. The pure PC and PC alloys all showed sharp glass-to-rubbery transitions.
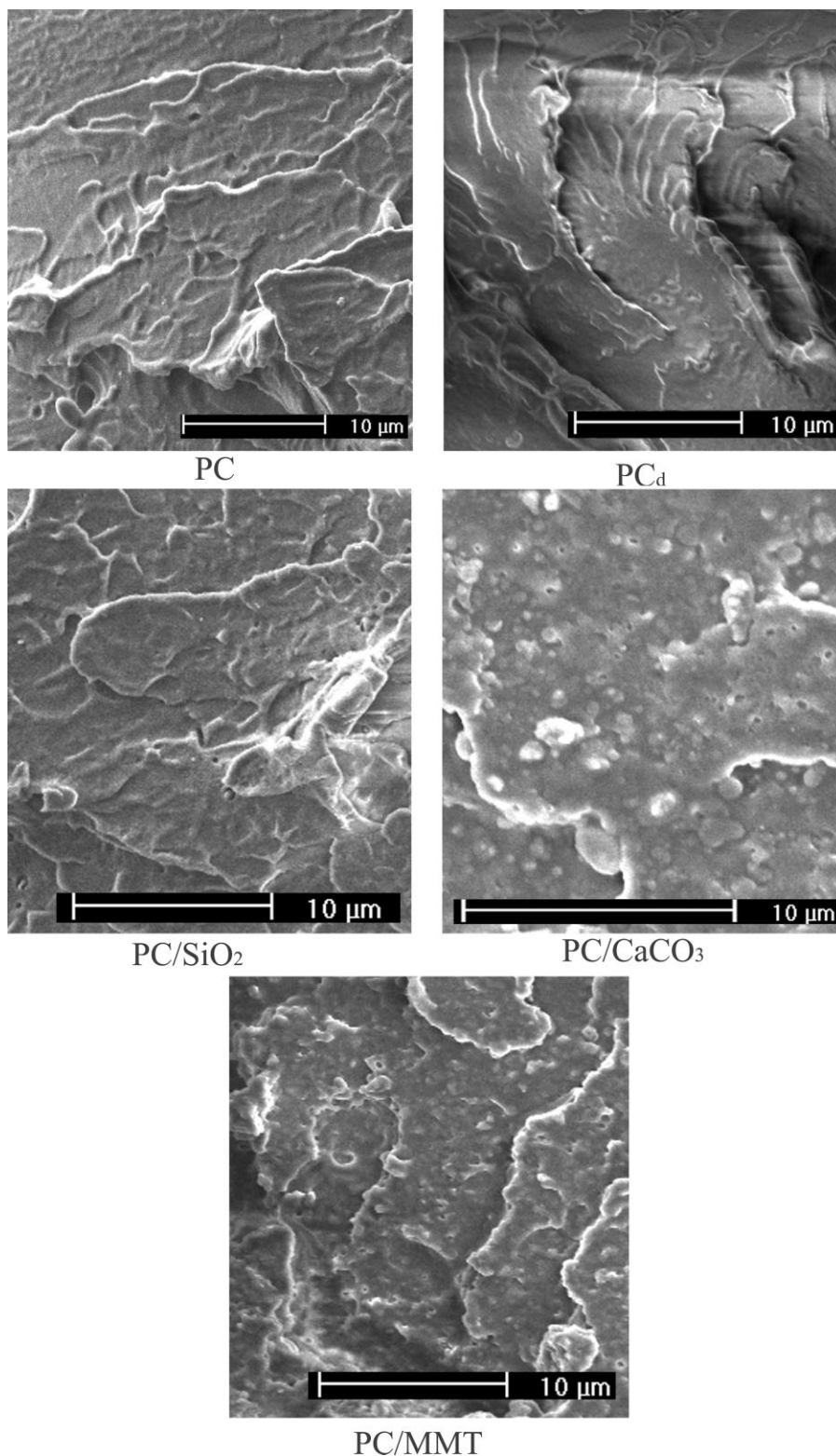

PC

PC$_d$

PC/SiO$_2$

PC/CaCO$_3$

PC/MMT

Figure 9 SEM micrographs of the PC and PC alloys.

Figure 7 shows the dynamic loss modulus (G'') of the PC and PC alloys. The peak strength in the G'' curve indicates the weight fraction of the phases in the polymer blends. The PC alloys showed two peaks at 20 and 150°C, which indicated the weight fractions of the rubber elastomers and PC, respectively. Through the addition of the rubber elastomers to the PC, there was a decrease in the strength of the peak, and the peaks were broadened and shifted to the lower temperature. For the PC alloys, the peaks were almost unchanged. The loss factor (tan δ) as a function of temperature for the PC alloys is shown in Figure 8. Pure PC showed a tan δ peak at 167°C. With the addition of the modifier into the PC matrix, the new tan δ peaks shifted to lower temperatures.

Morphology

The particle size and distribution of the composite particles in the PC matrix were characterized with SEM, as shown in Figure 9. The inorganic nanoparticles encapsulated by thermoplastic acrylic acid ester polymers were well dispersed in the PC matrix and formed a cocontinuous phase.

Combustion

The combustion properties of the PC and PC alloys were characterized with a cone calorimeter. The HRR plots for PC/MMT, PC/SiO$_2$, PC/CaCO$_3$, PC$_d$, and PC at 35 kW/m^2 are shown in Figure 10. It shows that the HRR peak for the PC/MMT, PC/SiO$_2$, and PC/CaCO$_3$ nanocomposites was lower than that for PC and PC$_d$. This indicates that the addition of MMT, SiO$_2$, and CaCO$_3$ could reduce the HRR of the PC matrix. The reduction in the average HRR of the PC/MMT, PC/SiO$_2$, and PC/CaCO$_3$
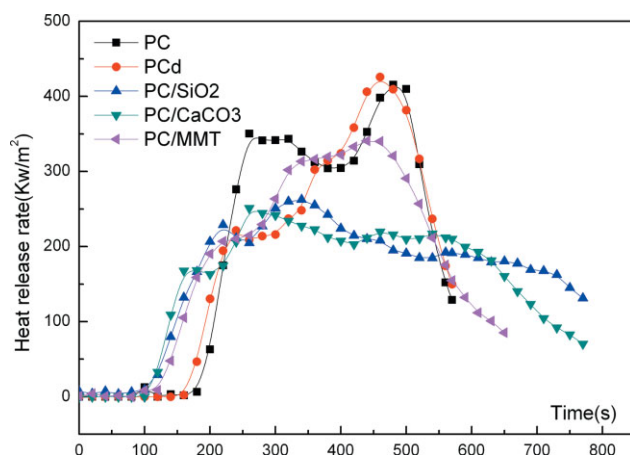

Figure 10 HRR plots for the pure PC and PC alloys at a heat flux of 35 kW/m^2. [Color figure can be viewed in the online issue, which is available at www.interscience.wiley.com.]

nanocomposites was 64, 62, and 13%, respectively. The influence of the MMT and SiO$_2$ particles on the combustion properties of PC was more effective than the influence of CaCO$_3$. This can be attributed to the fact that the particle size of MMT and SiO$_2$ is smaller than that of CaCO$_3$; as a result, the MMT and SiO$_2$ particles functioned better as barriers than CaCO$_3$ in the PC matrix. As shown in Figure 10, these PC alloys had a shorter ignition time and a longer burning time than PC and PC$_d$; this indicates that the addition of MMT, SiO$_2$, and CaCO$_3$ could accelerate the ignition of the PC matrix.

Characterization of the char surface

Figure 11 presents scanning electron micrographs of the PC and PC alloys. According to the figure, the sample of PC was incompact and could not form an insulating layer, and there were many wrinkles and cracks in PC/CaCO$_3$. At the same time, PC/MMT and PC/SiO$_2$ were smoother and more compact than PC/CaCO$_3$ and PC$_d$. The small particles of MMT and SiO$_2$ accumulated to form an insulating layer on the surface, and this further confirmed that the MMT and SiO$_2$ particles aggregated on the surface during burning, preventing the transfer of heat and mass. The reason is that the quantity of nanoparticles was small (ca. 1%) in the PC alloys, but the nanoparticles were very small; the diameter of the nanoparticles was 200 nm. The sample surface (200 nm × 100 = 20 μm) of the PC alloys should have had a nanoparticle layer. These particles aggregated on the surface, preventing heat and mass transfer during burning.

CONCLUSIONS

PC was blended with modifiers containing different inorganic nanoparticles with a twin-screw extruder. In comparison with pure PC, the melt viscosity of the blends decreased, and this resulted in a reduction of the processing temperature. The mechanical performance testing showed that the impact strength and the bending strength and tensile modulus of the PC alloys was improved and reduced, respectively, in comparison with those of PC; this is different from the results reported in previous works. The improvement of the impact strength was attributed to the fact that the alloys had a new absorbing peak at lower temperatures, and this was confirmed by dynamic mechanical analysis.

The flammability properties of PC filled with MMT, SiO$_2$, and CaCO$_3$ were also investigated with a cone calorimeter and a scanning electron microscope. The results suggest that the inorganic particles form an insulating layer on the surface during burning and can prevent the transfer of heat and
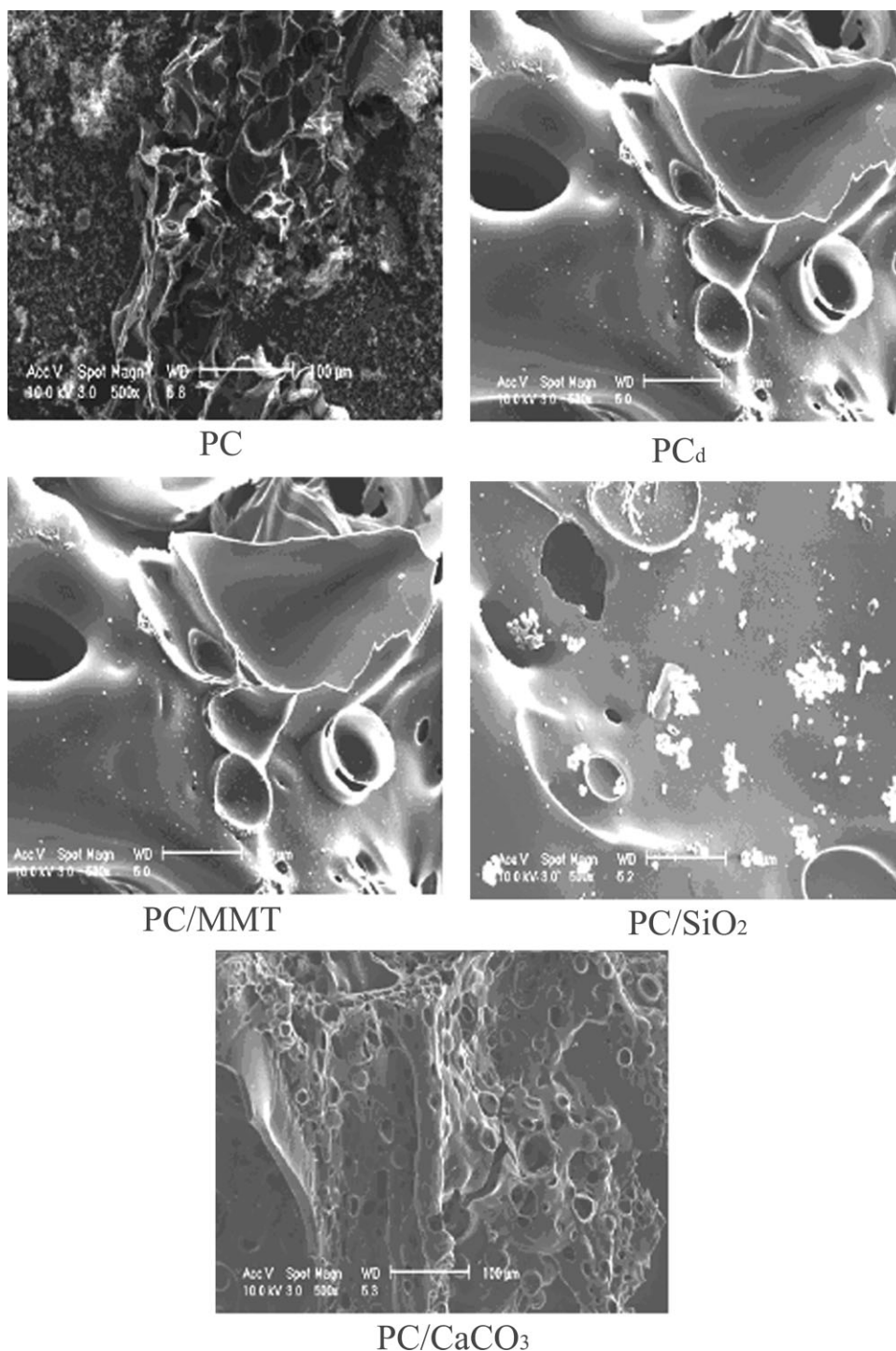
Figure 11 SEM micrographs of the PC and PC alloys.

mass. In comparison with $CaCO_3$, MMT and SiO_2 have worse flammability because they are smaller than $CaCO_3$.

References

1. Bucknall, C. B. Toughened Plastics; Applied Science: London, 1977.

2. Collyer, A. A. Rubber Toughened Engineering Plastics; Chapman & Hall: London, 1994.

3. Chang, F.-C.; Wu, J.-S.; Chu, L.-H. J Appl Polym Sci 1992, 44, 491.

4. Deanin, R. D. Concise Polymeric Materials Encyclopedia; CRC: Boca Raton, FL, 1999, 13.

5. Freitag, D.; Grigo, V.; Müller, P. R.; Nouvertne, W. Encyclopedia of Polymer Science and Engineering; Wiley: New York, 1990; Vol. 11, p 28.

6. Maxwell, M. A.; Yee, A. F. Polym Eng Sci 1981, 21, 205.

7. Wang, X.-H.; Wang, Z.-G.; Jiang, W.; Liu, C.-H.; Zhang, H.-D.; Zhang, H.-X.; Jiang, B.-Z. Polymer 1997, 38, 6251.

8. van der Sanden, M. C. M.; de Kok, J. M. M.; Meijer, H. E. H. Polymer 1994, 35, 2995.

9. Lee, M.-P.; Hiltner, A.; Baer, E. Polymer 1992, 33, 675.

10. Lee, M.-P.; Hiltner, A.; Baer, E. Polymer 1992, 33, 685.

11. Inberg, J. P. F.; Gaymans, R. J. Polymer 2002, 43, 2425.

12. Inberg, J. P. F.; Takens, A.; Gaymans, R. J. Polymer 2002, 43, 2795.

13. Inberg, J. P. F.; Gaymans, R. J. Polymer 2002, 43, 3767.

14. Inberg, J. P. F.; Gaymans, R. J. Polymer 2002, 43, 4197.

15. Ishikawa, M.; Chiba, I. Polymer 1990, 31, 1232.

16. Hansen, M. G.; Bland, D. G. Polym Eng Sci 1985, 25, 896.

17. Falk, J. C.; Narducy, K. W.; Cohen, M. S.; Brunner, R. Polym Eng Sci 1980, 209, 763.

18. Ohishi, H.; Ikehara, T.; Nishi, T. J Appl Polym Sci 2001, 80, 2347.

19. Riew, C. K.; Smith, R. W. In Rubber-Toughened Plastics; Riew, C. K., Ed.; Advances in Chemistry; American Chemical Society: Washington, DC, 1989; p 222.

20. Parker, D. S.; Jue, H.-S.; Huang, J.; Yee, A. F. Polymer 1990, 31, 2268.

21. Cheng, T. W.; Keskkula, H.; Paul, D. R. J Appl Polym Sci 1992, 45, 531.

22. Kayano, Y.; Keskkula, H.; Paul, D. R. Polymer 1998, 39, 821.

23. Cheng, C.; Hiltner, A.; Baer, E.; Soskey, P. R.; Mylonakis, S. G. J Appl Polym Sci 1994, 52, 177.

24. Cheng, C.; Peduto, N.; Hiltner, A.; Baer, E.; Soskey, P. R.; Mylonakis, S. G. J Appl Polym Sci 1994, 53, 513.

25. Cheng, C.; Hiltner, A.; Baer, E.; Soskey, P. R.; Mylonakis, S. G. J Appl Polym Sci 1995, 55, 1691.

26. Fambri, L.; Penati, A.; Kolarik, J. Polymer 1998, 38, 835.

27. Palanivelu, K.; Sivaraman, P.; Sharma, S. K. Plast Technol 2002, 5, 36.

28. Lee, K. J.; Jim, J. M.; Kum, J. G.; Oh, J. M. SPE Annu Tech Conf 1998, 98, 2458.

29. Sivaraman, P. Polym Test 2004, 23, 645.

30. Perepechko, I. Acoustic Methods of Investigating Polymers; Mir: Moscow, 1975.